Axicon lens for high-resolution optical coherence tomography over a long focus depth

Zhihua Ding, Hongwu Ren, Yonghua Zhao, J. Stuart Nelson and Zhongping Chen
Beckman Laser Institute, University of California, Irvine CA 92612

ABSTRACT

In optical coherence tomography (OCT), axial and lateral resolutions are determined by the source coherence length and numerical aperture of the sampling lens, respectively. While axial resolution can be improved using a broadband light source, there is a trade-off between lateral resolution and focus depth when conventional optical elements are used. In this paper, we report on the incorporation of an axicon lens into the sample arm of the interferometer to overcome this limitation. Using an axicon lens with a top angle of 160 degrees, 10 μm or better lateral resolution is maintained over a focus depth of at least 6 mm. In addition to high lateral resolution, the focusing spot intensity is approximately constant over the whole focus depth.

Keywords: Optical coherence tomography (OCT), axicon lens, focus depth, lateral resolution

1. INTRODUCTION

Optical coherence tomography (OCT) is a new modality that provides high resolution subsurface microstructural images in a noninvasive manner [1, 2]. OCT uses coherence gating to select minimally scattered photons for image reconstruction. Axial and lateral resolutions are determined by the source coherence length and numerical aperture of the sampling lens, respectively. While axial resolution can be improved using a broadband light source [3, 4], there is a trade-off between lateral resolution and focus depth when conventional optical elements (spherical lenses, mirrors, etc.) are used, because a beam with a long focus depth and narrow lateral width cannot be produced simultaneously. While high lateral resolution imaging requires a large numerical aperture, a long focus depth requires a small numerical aperture. In high speed OCT imaging, where an axial scanning mode (A-mode) is used, a tightly-focused lens produces a micrometer sized spot at only one particular depth. The coherence gate quickly moves out of the short focus depth during the scan. Although dynamic focusing compensation [3, 4, 5] can be used to overcome this limitation, current lenses can only be used at low speeds, which limits their use in low frame rate OCT systems. In addition, dynamic focusing lenses are bulky and cannot be implemented in circumstances where physical space is limited such as endoscopic OCT [6, 7].

In this paper, an axicon lens [8] is incorporated into the sample arm of the interferometer to achieve both high lateral resolution and long focus depth simultaneously. The 'axicon' was first introduced by McLeod [8], as a term to describe an optical element that produces a line image lying along the axis from a point source of light. There are many different kinds of axicon (rings, cylinders, and etc.), but the single refracting cone lens is the most common form. Hereafter in this paper we refer an axicon lens specifically to a refracting conical lens. Using an axicon lens with a top angle of 160 degrees, 10 μm lateral resolution or better is maintained over a focus depth of at least 6 mm. In addition to high lateral resolution, the focusing spot intensity is approximately constant over the whole focus depth.

2. METHODOLOGY

A high speed phase-resolved OCT system at 1.3 μm is used in our experiments. A detailed system design has already been described in the literature [9]. We incorporate an axicon lens into the sample arm of the interferometer. A schematic of the interferometer with a fused silica axicon lens (1 inch diameter, top angle of 160 degrees, AR coating 1050-1350 nm, edge thickness 3 mm, and diffraction index of 1.44681 at wavelength of 1.3 μm) is shown in Figure 1.

Coherence Domain Optical Methods in Biomedical Science and Clinical Applications VI,
Valery V. Tuchin, Joseph A. Izatt, James G. Fujimoto, Editors, Proceedings of SPIE
Vol. 4619 (2002) © 2002 SPIE · 1605-7422/02/$15.00

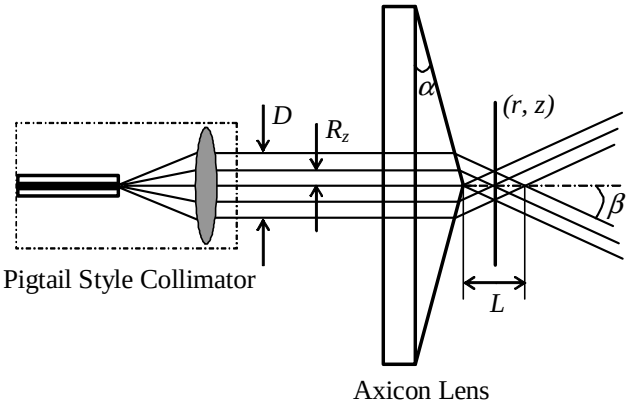

Fig. 1. Schematic of the sample arm in the OCT system using an axicon lens to achieve both high lateral resolution and long focus depth simultaneously. α: the angle formed by the conical surface with the flat surface of the axicon lens; β: the intersection angle of geometrical rays with the optical axis; R_z; radius of incident beam; D: waist of incident beam; L: depth of focus.

Light emitting from a single mode fiber is collimated with a lens to produce a spatially coherent illumination upon the axicon lens. Spatially coherent illumination is necessary for the axicon lens to produce a coherent and sharply focused spot. If spatially incoherent light illumination is used, the spot becomes wider and spatially incoherent [10], resulting in reduced transverse resolution and low signal to noise ratio (SNR) in OCT. The intensity distribution, *I(r,z)*, behind the axicon lens illuminated by a collimated beam of diameter *D* is given by [11]

$$I(r,z) = E^2(R_z)R_z \frac{2\pi k \sin\beta}{\cos^2\beta} J_0^2(kr\sin\beta),\ R \le D/2,\ z \le L \tag{1}$$

where $E^2(R_z)$ is the energy of the incident beam at radius R_z contributing to the intensity at axial point *z* through the relationship:

$$R_z = \frac{z\tan\beta}{1-\tan\alpha\tan\beta} \tag{2}$$

k is the wave number, J_0 is the zero-order Bessel function of the first kind, *r* is the radial coordinate on the observation plane, and *L* is the focus depth approximated by

$$L = \frac{D(\tan^{-1}\beta - \tan\alpha)}{2} \tag{3}$$

$\beta = \sin^{-1}(n\sin\alpha) - \alpha$, the intersection angle of geometrical rays with the optical axis is deduced from Snell's law and takes the form

$$n\sin\alpha = \sin(\alpha+\beta) \tag{4}$$

where *n* is the refraction index of the axicon lens and α is the angle formed by the conical surface with the flat surface of the axicon lens. According to Eq. 1, the central peak radius, ρ_0, of the beam behind the axicon lens can be predicted by the first zero of the Bessel function

$$J_0(k\rho_0\sin\beta) = 0 \tag{5}$$

which results in

$$\rho_0 = \frac{2.4048\lambda}{2\pi\sin\beta} \tag{6}$$

Inserting the relevant parameters pertaining to the axicon lens (α=10 degrees, *D*=2 mm, λ=1.3 μm and *n*=1.44681) into Eqs. 3 and 6, the estimated focus depth *L* is 12.4 mm and the central peak radius ρ_0 is 6.32 μm.

3. EXPERIMENTS

To test our OCT system performance, we first measured the detected signal versus mirror axial position behind the axicon lens by blocking out the reference arm and using a reflecting mirror as the sample (Figure 2). For comparison, signal versus axial position of a conventional lens (f=10 mm, NA=0.35, WD=6.8 mm) replacing the axicon lens shown in Figure 1 is also measured. The result clearly demonstrates that the axicon lens has a much longer focus depth than the conventional lens. The focus depth is approximately 7 mm (full width at $1/e^2$), which is smaller than the theoretical value of 12 mm. The reason for the reduced focus depth is that the spherical geometrical shape of the axicon apex acts as an equivalent lens and focuses the central part of the illuminating light to a point away from the axicon apex. Because focal energy using an axicon lens is distributed along a much longer focus depth, the power at each focusing point using an axicon lens is smaller than that using a conventional focusing lens. In Figure 2, the detected peak signal ratio between the conventional and axicon lenses is about 16. There is a compromise between signal intensity and focus depth. However, our current system using an over the counter axicon lens has a focus depth of more than 6 mm. If an axicon lens designed specifically for OCT is made with a focus depth of 2 mm, the difference in peak intensity between the axicon and conventional lenses will be much reduced.

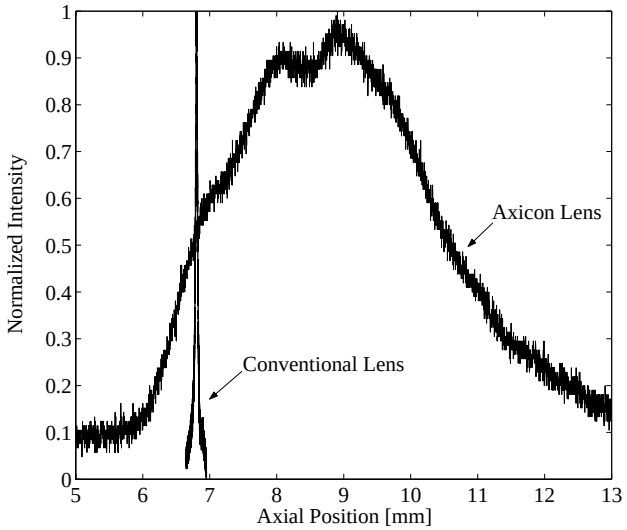

Fig. 2. Signal versus axial position in the sample arm of the interferometer.

The focus depth and lateral resolution of the axicon lens based OCT system was calibrated with a variable frequency resolution target from Edmund Scientific (Barrington, NJ). Sequences of OCT images were made with the target located at different axial positions. The density of the parallel bar to be imaged was 50 line pairs per mm, which corresponds to a spatial resolution of 10 μm. Figure 3 shows the OCT images and their corresponding cross-sectional profiles for the target located at different axial positions relative to the axicon apex with an interval of 1.2 mm over a total observed depth of 6 mm. The OCT image size is 600 μm by 200 μm. These results confirm a focus depth of at least 6 mm with 10 μm or better lateral resolution. In contrast, the Rayleigh range for a TEM_{00} Gaussian beam with a 10 μm waist radius at a wavelength of 1.3 μm is less than 0.25 mm.

To confirm the feasibility of the axicon lens based OCT system, images were taken of the same sample with both axicon and conventional lenses. The sample is polystyrene microspheres (diameter=0.356 μm) inside a capillary tube immersed in water. The internal diameter of the tube is 1.1 mm and the wall thickness is 0.20 mm. The 2.7% polystyrene microsphere solution was diluted with distilled water at volume ratio of 1 to 10 (scattering coefficient calculated to be 4.8 cm^{-1}). An OCT image using an axicon lens is shown in Figure 4A where both the lumen and tube wall can be observed; image size is 2 mm by 2 mm. An OCT signal as a function of depth plotted across the center of the lumen is

shown in Figure 4A′. Although a slow decay in the signal is observed as a function of depth, this decay is mainly due to scattering attenuation by the microspheres. For comparison, OCT images using a conventional lens for different focusing positions in the lumen are shown in Figures 4B and 4C. The bright region corresponds to the focusing location of the lens. Plots of the corresponding signals as a function of depth (Figures 4B′ and 4C′) when compared to Figure 4A′, clearly indicate that the signals are strongly dependent on the focusing locations. The OCT signal decays much faster away from the focus. Thus, in addition to high lateral resolution over a longer focus depth, the OCT signal is more uniform over the whole focus depth when using an axicon lens.

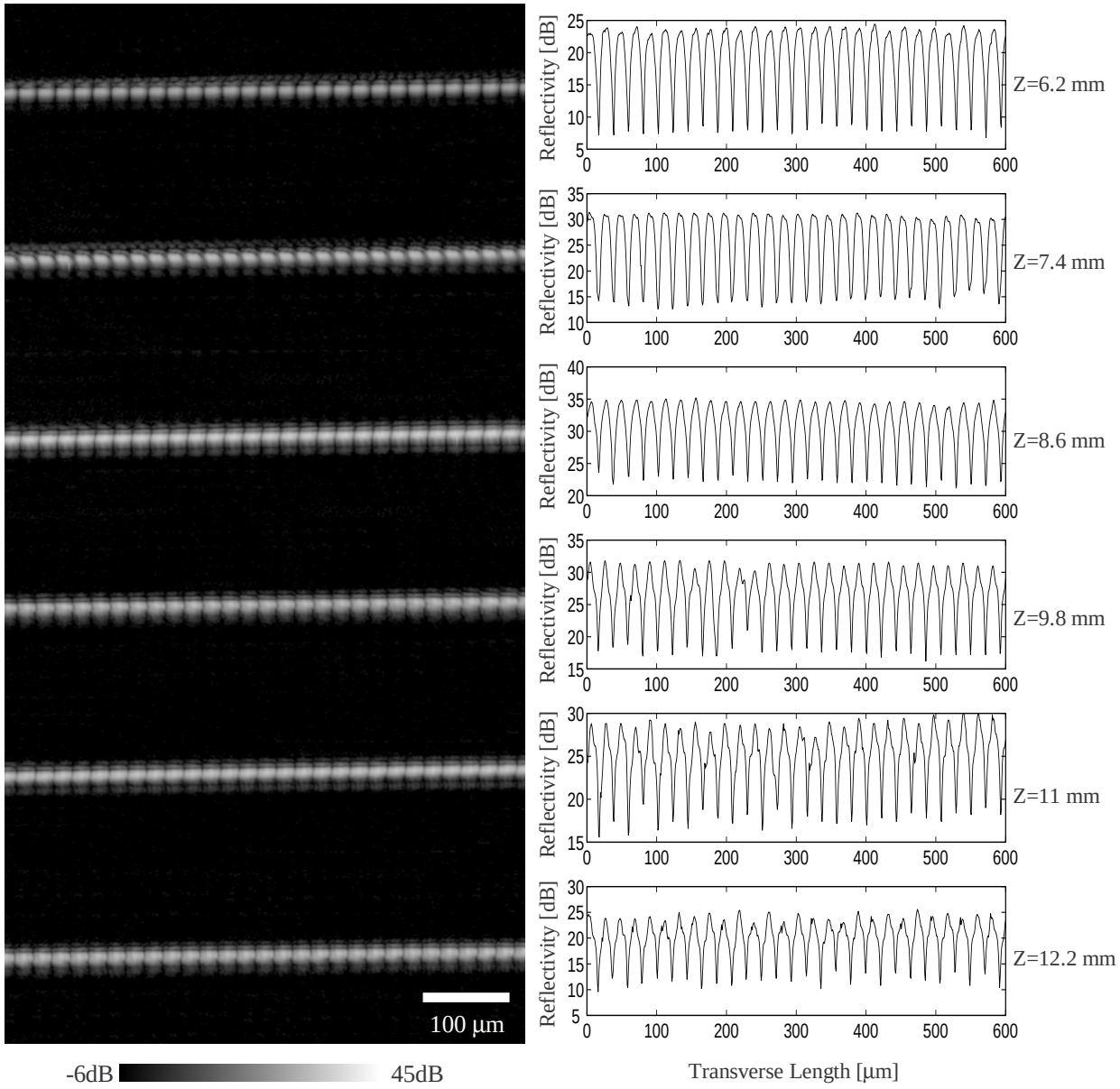

Fig. 3. OCT images and their cross-sectional profiles normal to the bar direction (noise floor is about -6 dB). Successive images from top to bottom correspond to the target located at different axial positions relative to the axicon apex with an interval of 1.2 mm over a total observed depth of 6 mm.

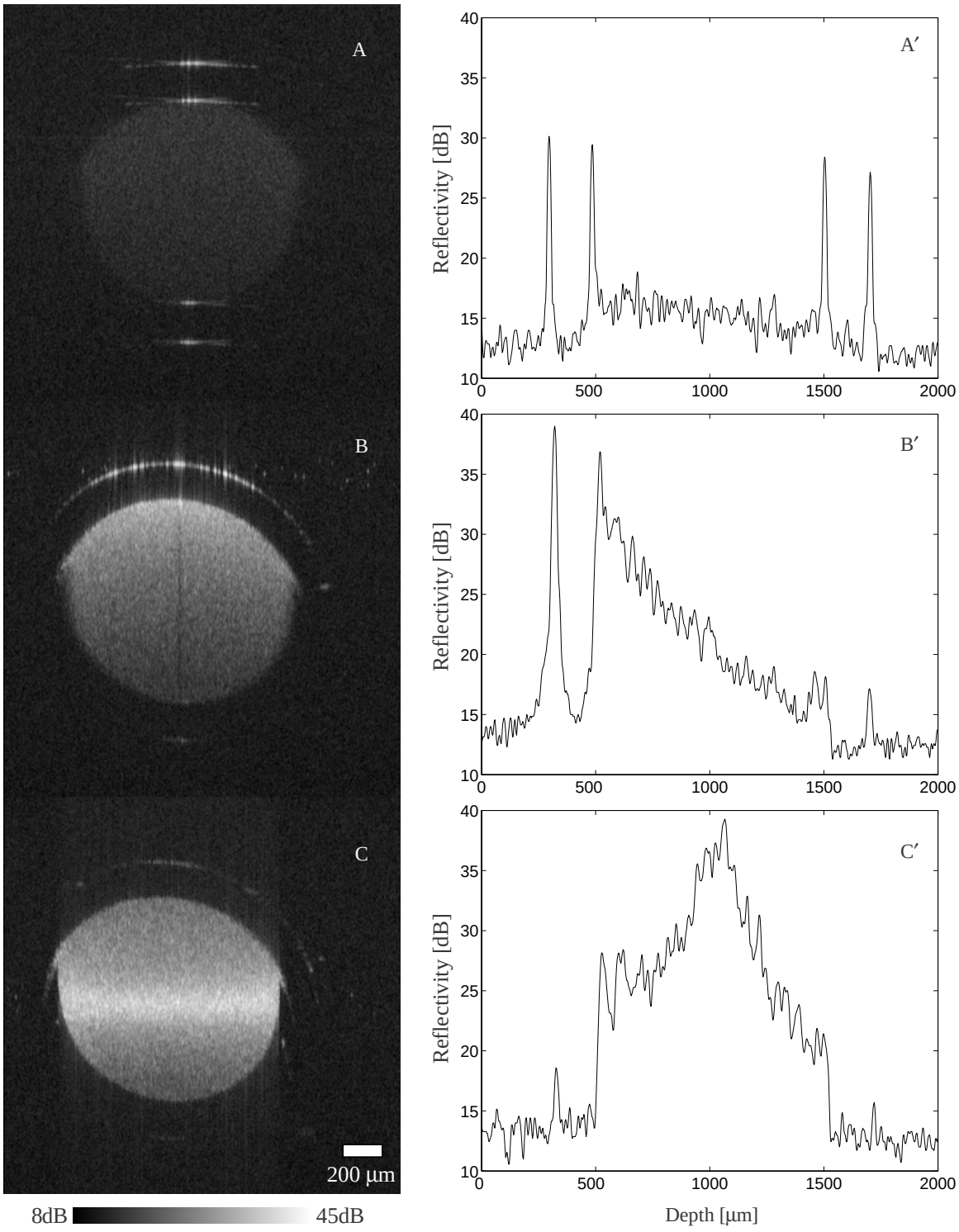

Fig. 4. OCT images of a capillary tube with polystyrene microspheres and their profiles along the center of the tube in the depth direction corresponding to different focusing locations in the sample. (A and A′) axicon lens; (B and B′) conventional lens focusing at the top of the tube; and (C and C′) conventional lens focusing at the center of the tube.

4. CONCLUSION

In conclusion, we have achieved 10 μm or better lateral resolution over a focus depth of at least 6 mm using an axicon lens with a top angle of 160 degrees in our OCT system. These results demonstrate that an axicon lens can be used in an OCT system to maintain high lateral resolution over a long focus depth, which is essential for high resolution, high-speed OCT.

ACKNOWLEDGEMENTS

This work was supported by research grants awarded from the National Institutes of Health (HL-64218, RR-01192 and GM-58785) and National Science Foundation (BES-86924). Institutional support from the Air Force Office of Scientific Research (N00014-94-1-0874), Department of Energy (DE-FG03-91ER61227) and the Beckman Laser Institute Endowment are also gratefully acknowledged. Correspondence should be addressed to Dr. Chen at zchen@bli.uci.edu.

REFERENCES

1. D. Huang, E. A. Swanson, C. P. Lin, J. S. Schuman, W. G. Stinson, W. Chang, M. R. Hee, T. Flotte, K. Gregory, C. A. Puliafito and J. G. Fujimoto, Science **254**, 1178 (1991).
2. Z. Chen, Y. Zhao, S. M. Srinivas, J. S. Nelson, N. Prakash and R. D. Frostig, IEEE J. Select. Topics in Quantum Electron. **5**, 1134 (1999).
3. W. Drexler, U. Morgner, F. X. Krtner, C. Pitris, S. A. Boppart, X. D. Li, E. P. Ippen and J. G. Fujimoto, Opt. Lett. **24**, 1221 (1999).
4. I. Hartl, X. D. Li, C. Chudoba, R. K. Ghanta, T. H. Ko, J. G. Fujimoto, J. K. Ranka and R. S. Windeler, Opt. Lett. **26**, 608 (2001).
5. Z. Chen, T. E. Milner, D. Dave and J. S. Nelson, Opt. Lett. **22**, 64 (1997).
6. G. J. Tearney, S. A. Boppart, B. E. Bouma, M. E. Brezinski, N. J. Weissman, J. F. Southern, and J. G. Fujimoto, Opt. Lett. **21,** 543 (1996).
7. A. M. Rollins, R. U.-Arunyawee, A. Chak, C. K. Wong, K. Kobayashi, M. V. Sivak and J. A. Izatt, Opt. Lett. **24**, 1358 (1999).
8. J. H. McLeod, J. Opt. Soc. Am. **44**, 592 (1954).
9. Y. Zhao, Z. Chen, C. Saxer, S. Xiang, J. F. de Boer and J. S. Nelson, Opt. Lett. **25**, 114 (2000).
10. A. T. Friberg and S. Y. Popov, Appl. Opt. 35, 3039 (1996).
11. R. M. Herman and T. A. Wiggins, J. Opt. Soc. Am. A **8**, 932 (1991).